Coverage Properties of the Target Area in Wireless Sensor Networks

Xiaoyun Li, *Member, IEEE,* David K. Hunter, *Senior Member, IEEE,* and Sergei Zuyev

***Abstract*—An analytical approximation is developed for the probability of sensing coverage in a wireless sensor network with randomly deployed sensor nodes each having an isotropic sensing area. This approximate probability is obtained by considering the properties of the geometric graph, in which an edge exists between any two vertices representing sensor nodes with overlapping sensing areas. The principal result is an approximation to the proportion of the sensing area that is covered by at least one sensing node, given the expected number of nodes per unit area in a two-dimensional Poisson process. The probability of a specified region being completely covered is also approximated. Simulation results corroborate the probabilistic analysis with low error, for any node density. The relationship between this approximation and non-coverage by the sensors is also examined. These results will have applications in planning and design tools for wireless sensor networks, and studies of coverage employing computational geometry.**

***Index Terms*—coverage, dimensioning, Poisson process, sensor networks, geometric graph.**

I. Introduction

A wireless sensor network (WSN) monitors some specific physical quantity, such as temperature, humidity, pressure or vibration. It collates and delivers the sensed data to at least one sink node, usually via multiple wireless hops. To ensure *sensing coverage*, the subject of this paper, the WSN must sense the required physical quantity over the entire area being monitored — while doing this, both power consumption and the efficiency of data aggregation are crucial considerations.

We assume ideal conditions where each sensor node has an isotropic sensing area defined by a circle of radius R, although in practice it may be directional to some extent because of physical obstacles. Although the analysis could be extended to cope with scenarios where a node's sensing range depends on the environment, the results in this paper nevertheless have practical significance for many deployments. They will be useful when estimating the sensor density required, or when determining the likelihood of holes in the sensing coverage. It is also assumed that the distribution of sensor nodes over the target sensing area is described by a homogeneous Poisson process, suggesting that the results are most relevant to applications with randomly scattered nodes.

X. Li is with: Shenzhen Institute of Advanced Technology, Chinese Academy of Sciences, 1068 Xueyuan Boulevard, University Town of Shenzhen, 518055, China. E-mail: xy.li@siat.ac.cn

D. K. Hunter is with: School of Computer Science and Electronic Engineering, University of Essex, Colchester CO4 3SQ, UK. E-mail: dkhunter@essex.ac.uk

S. Zuyev is with: Department of Mathematical Sciences, Chalmers University of Technology, SE-412 96 Gothenburg, Sweden. E-mail: sergei.zuyev@chalmers.se

A point in the plane is said to be *tri-covered* if it lies inside some triangle formed by three edges in the *geometric graph*. In this graph, each active sensor node is represented by a vertex, and an edge exists between any two vertices representing nodes with overlapping sensing areas; with the isotropic coverage assumed here, this happens when the corresponding nodes are less than $2R$ units apart (Figure 1). The clustering and graph partitioning properties of geometric graphs have already been investigated [1]–[3], with applications for example in the design of frequency partitioning algorithms for wireless broadcast networks. Furthermore, an area is said to be tri-covered if every point within it is tri-covered. A bound is determined for the probability that all points in the target area which are further than R units from its boundary are tri-covered.

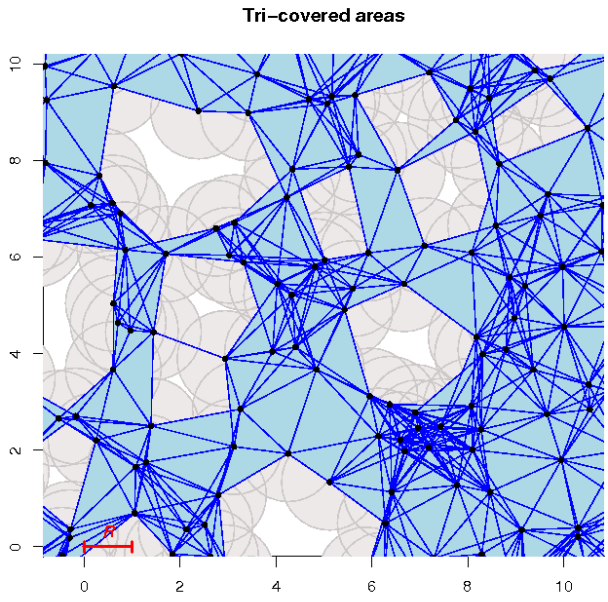

Fig. 1. A portion of the target area with $\lambda = 1$ and $R = 1$; nodes closer than $2R$ units to one another are connected by edges, and the shaded areas contain only points which are tri-covered. The circular sensing range of each sensor node is also shown.

Tri-coverage is closely related to sensing coverage. If an area is not tri-covered, there must be points inside it which are not covered by the sensing area of any node (white space in Figure 1); see the proof in Section IV. The connected components of areas which are not tri-covered are called

large holes. However, a point may still be tri-covered, but nevertheless not be covered by any node's sensing area, as in Figure 2. Such points are said to lie inside a *trivial hole*. An estimate obtained below shows that the proportion of space in homogeneous systems occupied by trivial holes is less than 0.03% regardless of the sensor node density, so they can in practice be ignored when calculating coverage. Hence the analytical calculations for the probability of full tri-coverage proposed here provide a good approximation to the real probability of sensing coverage, albeit in an idealised scenario, although no assumptions are made about the shape of the overall area to be covered. This will be a useful guide for making network planning and design decisions, especially as our analytical method generates results much more quickly than can be achieved by simulation.

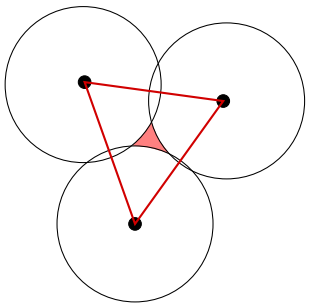

Fig. 2. A trivial hole; the central shaded area lies inside a triangle defined by the graph but is nonetheless not covered.

The coverage problem for sensor networks has been investigated in previous studies [4], [5], [6], with mathematical methods having been developed for the calculation or estimation of sensing coverage [7], [8], [9], [10]. Although tri-coverage provides a useful way of approximating overall coverage, the analysis presented here using the geometric graph is also directly relevant to a general class of distributed algorithms which use only local connectivity information in order to determine the extent of coverage; for examples see [11] and [12].

II. Probabilistic Model

The usual assumption is made that the sensor nodes are distributed in the plane according to a homogeneous Poisson process with intensity λ so that on average there are λ nodes per unit of space. Because of homogeneity, each point in space has an equal chance of being tri-covered, so the probability that the origin O is tri-covered will be considered. This probability in a homogeneous setting equates to the proportion of the space which is tri-covered, which is a key parameter to be considered when designing WSNs.

Because the lengths of each edge of the triangle covering O must be at most $2R$, only the nodes within $2R$ units from the origin can contribute to tri-coverage of O. Hence this probability depends, in fact, on the restriction of the Poisson process onto the closed ball $b(O, 2R)$ of radius $2R$ centered at the origin which is also a finite homogeneous Poisson process with intensity λ; this process is denoted by Π. It is convenient to treat Π as a counting measure, so that $\Pi(B)$ denotes the number of nodes in a set B. Because zooming into the realisation a times increases the sensing radius a times while decreasing the node density by a factor of a^2, without changing the geometry and hence the property of tri-coverage, the probability of tri-coverage is a function only of the dimensionless parameter λ/R^2. For this reason, $R = 1$ is assumed below, remembering that the bounds derived below (which are functions of λ) should be applied to λ/R^2 if $R \neq 1$.

III. Bounds on Probability of Tri-coverage

Denote by $T(x, y, z)$ the property that three points x, y, z are at a distance not exceeding 2 $(= 2R)$ from each other, and the triangle with these points as vertices covers the origin. With a slight abuse of notation, when x_0, x_1, x_2 are nodes in the process Π, $T(x_0, x_1, x_2)$ is also written to denote the *event* that the nodes x_0, x_1 and x_2 cover the origin with a triangle.

Let $\xi_0 = \xi_0(\Pi)$ be the node within configuration Π which is closest to the origin. With the convention that the union is empty if there are fewer than three nodes in the process Π, the following can be written:

$$\begin{aligned} p(\lambda) &\stackrel{\text{def}}{=} \mathbf{P}\{O \text{ is tri-covered}\} \\ &= \mathbf{P}\Big\{ \bigcup_{\{x_0,x_1,x_2\}\subseteq\Pi} T(x_0, x_1, x_2)\Big\} \\ &> \mathbf{P}\Big\{ \bigcup_{\{x_1,x_2\}\subseteq\Pi\setminus\{\xi_0(\Pi)\}} T(\xi_0, x_1, x_2)\Big\}. \end{aligned}$$

Although it is possible that ξ_0 does not contribute to the tri-coverage of O, as exemplified in Figure 3, these configurations are rare (simulations show that this happens in less than 0.5% of realisations, see Table I), so the lower bound above is actually quite accurate.

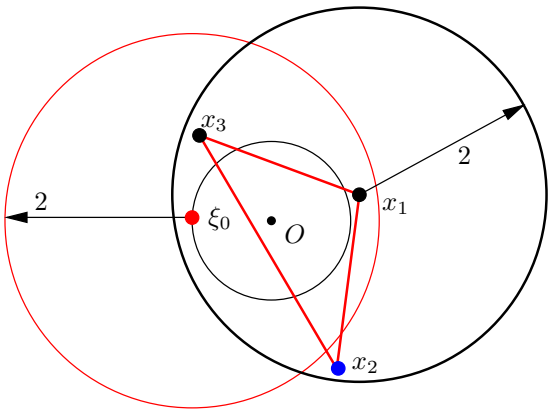

Fig. 3. Example of a configuration when the node closest to the origin ξ_0 does not contribute to tri-coverage because the distance to node x_2 exceeds 2 and the triangle $T(\xi_0, x_1, x_3)$ does not cover O. In contrast, $T(x_1, x_2, x_3)$ does cover O.

Now rotate the axes so that the closest node ξ_0 lies on the negative abscissa axis and thus has the new coordinates $(-\rho_0, 0)$. The distance ρ_0 to the closest node is a random variable with the distribution

$$F_{\rho_0}(r_0) = \mathbf{P}\{\rho_0 \leq r_0\} = 1 - e^{-\lambda\pi r_0^2}$$

because the event $\rho_0 > r_0$ is equivalent to the ball $b(0, r_0)$ not containing any nodes from the process, and is thus given by the Poisson probability $\exp\{-\lambda|b(0, r_0)|\}$, where $|B|$ stands for the area of the set B. Hence, the above lower bound can be written as

$$\mathbf{P}\Big\{\bigcup_{\{x_1,x_2\}\subseteq\Pi\setminus\{\xi_0(\Pi)\}} T(\xi_0, x_1, x_2)\Big\} = \int \mathbf{P}\Big\{\bigcup_{\{x_1,x_2\}\subseteq\Pi'_{r_0}} T((-r_0, 0), x_1, x_2)\Big\}\, F_{\rho_0}(dr_0)\,.$$

Π'_{r_0} above is the restriction of Π into $b(0, 2) \setminus b(0, r_0)$ which is again a Poisson process with intensity λ restricted to this domain. The strong Markov property of Poisson processes was used here; the random ball $b(0, \xi_0)$ is a *stopping set*, hence conditioning on its geometry (i.e. on its radius $\rho_0 = r_0$) implies that the process outside the stopping set is again Poisson, independent of the restriction of the process onto the stopping set. For details on stopping sets in the Poisson framework, see, e. g., [13] and [14].

If the origin is tri-covered with one of the nodes being $\xi_0 = (-\rho_0, 0)$, then the other two nodes necessarily lie in different half spaces: one in $H^+ = \mathbb{R} \times (0, \infty)$ and the other one in $H^- = \mathbb{R} \times (-\infty, 0)$. Moreover, because the distance to ξ_0 is less than 2, they both lie in the ball $b(\xi_0, 2)$ and they miss the ball $b(0, \rho_0)$ which must not contain any nodes by definition of ξ_0. The nodes in $H^+ \cap b(\xi_0, 2) \setminus b(0, \rho_0)$ are written in polar coordinates and ordered by increasing polar angle so that $\xi_1 = (\rho_1, \varphi_1)$ has the smallest polar angle φ_1, the next one is $\xi'_1 = (\rho'_1, \varphi'_1)$ with $\varphi'_1 > \varphi_1$ and so on until all the nodes are listed (Figure 4).

If the node ξ_1 participates in the tri-coverage together with ξ_0 and some $\xi_2 \in H^- \cap b(\xi_0, 2) \setminus b(0, \rho_0)$ then this ξ_2 must lie to the right of the line passing through ξ_1 and O, i.e. in the half-plane $H^+(\varphi_1)$ which consists of the points having the polar coordinates (r, φ) with $\varphi \in (\varphi_1 - \pi, \varphi_1)$. In addition, $\|\xi_1 - \xi_2\| \le 2$ so that ξ_2 lies in the figure

$$G^-(\xi_0, \xi_1) = G^-(\rho_0, \rho_1, \varphi_1) = H^- \cap b(\xi_0, 2) \setminus b(0, \rho_0) \cap H^+(\varphi_1) \cap b((\rho_1, \varphi_1), 2)\,.$$

It is easy to express the density of node ξ_1. The intensity measure of the Poisson process points in polar coordinates is $\lambda r dr d\varphi$, and because of the way ξ_1 was defined, there should be no nodes with a polar angle less than φ_1, i.e. no nodes in the set

$$G^+(\xi_0, \xi_1) = G^+(\rho_0, \varphi_1) = H^+ \cap b(\xi_0, 2) \setminus b(0, \rho_0) \cap H^+(\varphi_1)\,.$$

Therefore, the density F_{ξ_1} of ξ_1 in polar coordinates has the form

$$F_{\xi_1}(dr_1, d\varphi_1) = \lambda r_1 \exp\{-\lambda|G^+(\rho_0, \varphi_1)|\} dr_1 d\varphi_1\,. \qquad (1)$$

This is not a probability density; it integrates to $1 - \exp\{-\lambda|H^+ \cap b(\xi_0, 2) \setminus b(0, \rho_0)|\}$ which is complement of the probability that no nodes in $H^+ \cap b(\xi_0, 2) \setminus b(0, \rho_0)$ are present, hence no ξ_1 is defined and tri-coverage is not possible. The integration domain $D(\rho_0)$ in the space of parameters (ρ_1, φ_1)

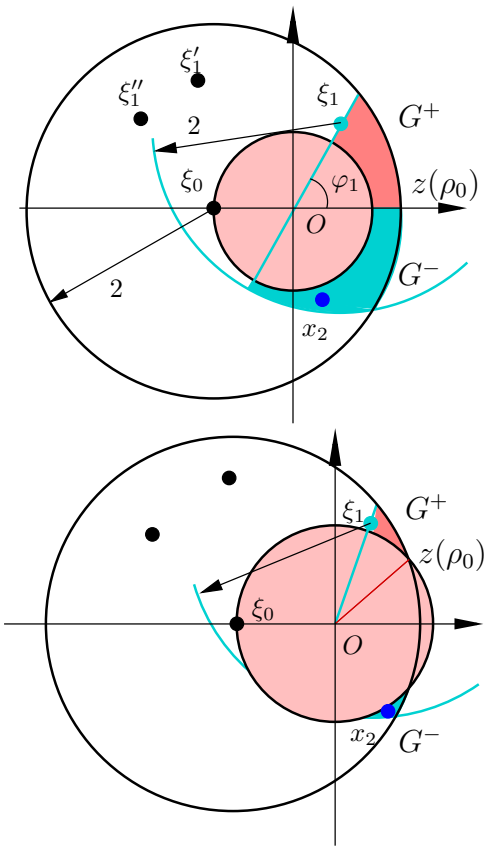

Fig. 4. Tri-coverage of the origin; there are no nodes in the area G^+ and there is at least one node in the area G^-.

depends on ρ_0; if $\rho_0 \le 1$ then the ball $b(0, \rho_0)$ is entirely inside $b(\xi_0, 2)$ (the upper diagram in Figure 4), and so $0 \le \varphi_1 \le \pi$ and $\rho_0 \le \rho_1 \le R_1$, where

$$R_1 = R_1(\rho_0, \varphi_1) = \sqrt{4 - \rho_0^2 \sin^2 \varphi_1} - \rho_0 \cos \varphi_1\,. \qquad (2)$$

If $1 < \rho_0 \le 2/\sqrt{3}$ (the lower diagram in Figure 4) then $2 \arccos(1/\rho) \le \varphi_1 \le \pi$ and it is still the case that $\rho_0 \le \rho_1 \le R_1$. It is easy to see that $G^-(\rho_0, \rho_1, \varphi_1)$ degenerates into a single point when $\rho_0 = 2/\sqrt{3}$ and becomes empty for larger ρ_0. So tri-coverage is not possible if $\rho_0 > 2/\sqrt{3}$.

Now a lower bound for the probability of tri-coverage can be expressed in an integral form. Noting that

$$\begin{aligned}&\mathbf{P}\Big\{\bigcup_{\{x_1,x_2\}\subseteq\Pi'_{r_0}} T((-r_0, 0), x_1, x_2)\Big\}\\ &> \iint_{D(r_0)} \mathbf{P}\Big\{\bigcup_{\substack{x_2\subseteq\Pi'_{r_0}\cap\\ G^-(r_0,r_1,\varphi_1)}} T\big((-r_0, 0), (r_1, \varphi_1), x_2\big)\Big\}\, F_{\xi_1}(dr_1, d\varphi_1)\\ &= \iint_{D(r_0)} \mathbf{P}\{\Pi'_{r_0}\big(G^-(r_0, r_1, \varphi_1)\big) > 0\}\, F_{\xi_1}(dr_1, d\varphi_1)\end{aligned} \qquad (3)$$

the following inequality may be derived:

$$p(\lambda) > p_0(\lambda) \stackrel{\text{def}}{=} 2\pi\lambda^2 \int_0^{2/\sqrt{3}} r_0 dr_0 \int_{z(r_0)}^{\pi} d\varphi_1 \int_{r_0}^{R_1(r_0,\varphi_1)} e^{-\lambda\pi r_0^2} \times e^{-\lambda|G^+(r_0,\varphi_1)|}\left(1 - e^{-\lambda|G^-(r_0,r_1,\varphi_1)|}\right) r_1 dr_1 \quad (4)$$

where $R_1(r_0, \varphi_1)$ is given by (2) and $z(r_0) = 0$ when $r_0 \le 1$, but $z(r_0) = 2\arccos(1/r_0)$ when $1 < r_0 \le 2/\sqrt{3}$.

When writing the above bound, Eq. (3) has been limited to tri-coverage involving node ξ_1 only. However, in principle the bound can be refined by including the situations where ξ_1 does not contribute to the tri-coverage, but the node $\xi_1' = (\rho_1', \varphi_1')$ with the next smallest polar angle $\varphi_1' > \varphi_1$ does (and even when ξ_1'' does, and so on). This situation is exemplified in Figure 5. If there is no node present in G^- there is still tri-coverage using ξ_1' provided there is a node x_2 in the set

$$G'^-(\rho_0, \rho_1, \varphi_1, \rho_1', \varphi_1') = G^-(\rho_0, \rho_1', \varphi_1') \setminus G^-(\rho_0, \rho_1, \varphi_1)\,.$$

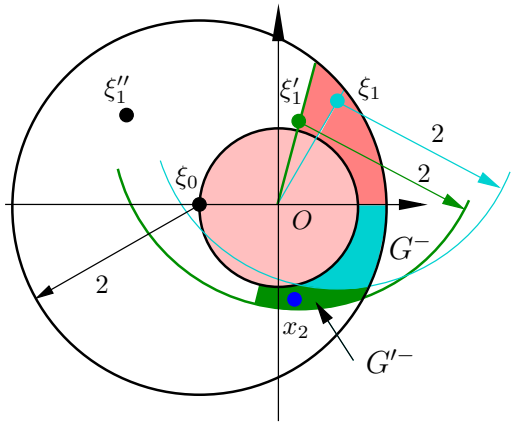

Fig. 5. The point ξ_1 with the smallest polar angle does not contribute to tri-coverage of the origin, but ξ_1' does; there is no node in G^- but there is a node in G'^-.

The density of the pair (ξ_1, ξ_1') is given by

$$F_{(\xi_1,\xi_1')}(dr_1, d\varphi_1, dr_1', d\varphi_1') = \lambda^2 r_1 r_1' \exp\{-\lambda|G^+(\rho_0, \varphi_1')|\} dr_1 d\varphi_1 dr_1' d\varphi_1'$$

and the right-hand side of the inequality (4) is complemented by the integral with respect to the following density:

$$e^{-\lambda|G^+(r_0,\varphi_1)|} e^{-\lambda|G^-(r_0,r_1,\varphi_1)|}\left(1 - e^{-\lambda|G'^-(r_0,r_1,\varphi_1,r_1',\rho_1')|}\right).$$

For most configurations the set G'^- is empty, therefore including such a term yields only a marginal improvement, so the bound (4) will be used from now on.

Although analytical expressions for $|G^+|$ and especially $|G^-|$ are rather cumbersome, they do not represent any problem for numerical evaluation of the integrals in (4) and it takes only a few seconds on an average laptop to compute the results with an accuracy of the order of 10^{-7}, compared to about an hour required for 10^6 simulations to obtain an order of 10^{-3} accuracy for the probability. Furthermore, this method for obtaining an analytic bound could be successfully adapted to more complex situations where, for example, nodes could adapt their sensing range depending on the environment.

All the computations and simulations were performed with the help of R, a software environment for statistical computing [15]. Technical details of the computation are not presented here, but they can be found in the R-code available from one of the authors' web-pages[1]. The idea is to represent the areas as a sum of sectors centered at the origin and spanned by the different points where balls $b(0, \rho_0)$, $b(\xi_0, 2)$ and $b(\xi_1, 2)$ intersect. For instance, the area $|G^+(r_0, \varphi_1)|$ in polar coordinates is expressed as the integral

$$\int_{z(r_0)}^{\varphi_1} d\varphi \int_{r_0}^{R_1(r_0,\varphi)} r\, dr = \frac{1}{2}\int_z^{\varphi_1} R_1^2(r_0, \varphi)\, d\varphi - \frac{1}{2} r_0^2(\varphi_1 - z(r_0))\,.$$

The first integral represents the area of the sector extending to the boundary of $b(\xi_0, 2)$ while the second represents the area of the sector extending to the boundary of $b(0, r_0)$. Also, the sectors are bounded by the ray φ_1 and z. z is either 0 as in the upper diagram in Figure 4, or $2\arccos(1/r_0)$, which is the polar angle of the intersection of circles $b(0, \rho_0)$ and $b(\xi_0, 2)$ in the upper half-plane as in the lower diagram. Similarly, the area of G^- can be computed, although additional cases having different geometries must be considered in addition to those shown in Figure 4; see Figure 6.

All these cases involve integrals of the type $\int_{\alpha_1}^{\alpha_2} R_{s_0,\alpha_0}^2(\varphi)\, d\varphi$, where

$$R_{s_0,\alpha_0}(\varphi) = \sqrt{4 - s_0^2 \sin^2(\varphi - \alpha_0)} + s_0 \cos(\varphi - \alpha_0)$$

is the equation of the circle of radius 2 centered at the point with polar coordinates (s_0, α_0). In this case the point (s_0, α_0) is either $(-r_0, \pi)$ or (r_1, φ_1). This integral has explicit form $I(\alpha_2 - \alpha_0) - I(\alpha_1 - \alpha_0)$, where

$$I(\alpha) = \frac{1}{2} s_0^2 \sin\alpha\cos\alpha + 2\alpha + 2\arcsin\left(\frac{1}{2} s_0 \sin\alpha\right) + \frac{1}{2} s_0 \sin\alpha \sqrt{4 - s_0^2 + s_0^2\cos^2\alpha}\,.$$

From this expression, and expressions for the angles of intersection of the different balls involved, explicit expressions follow for $|G^+|$ and $|G^-|$. Numeric evaluation of the triple integral yields the results presented in Table I and Figure 7. The simulation results presented in the table show that the difference between the bound (4) and the estimated probability of tri-coverage does not exceed 4% in absolute terms and 7% of the relative error, which is more than adequate for practical applications.

Remark 1. Motivated by sensor network applications, this paper has concentrated on obtaining a lower bound on the probability of tri-coverage, which enables estimation of the sensor node density necessary to guarantee acceptable sensing performance. However, an upper bound can easily be obtained through the following observation. Consider a triangle with edges not exceeding 2 units. The distance from any point

[1] www.math.chalmers.se/~sergei

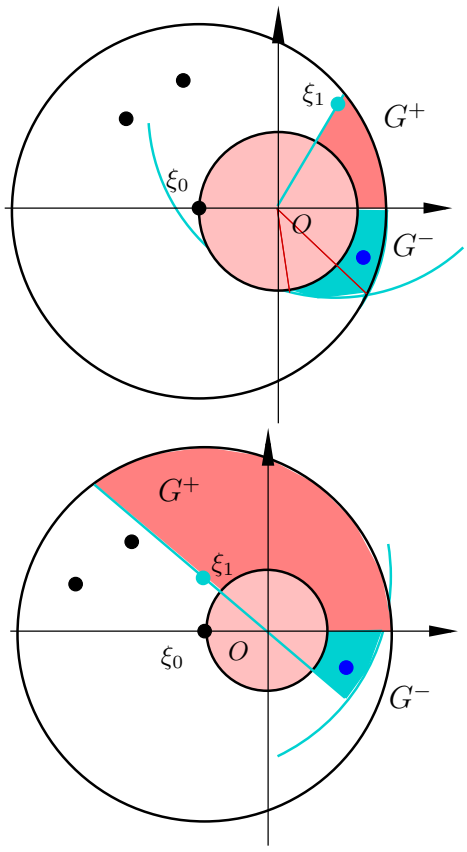

Fig. 6. Cases of different geometry of the set G^-.

inside this triangle to any vertex is at most 2, so the ball $b(O,2)$ contains at least three nodes when the origin is tri-covered. Therefore

$$p(\lambda) < 1 - (1 + 4\pi\lambda + 8\pi^2\lambda^2)\, e^{-4\pi\lambda} \tag{5}$$

However, further estimation of the probability of tri-coverage from the above equation is not pursued in this paper.

IV. Estimate of the Probability of Existence of an Area which is not Tri-covered

In this section bounds are derived on the probability that the whole of a 'large' sensing area B is tri-covered.

The sensing coverage of a convex set $B^R = B + b(O,R)$ by disks of radius R implies tri-coverage of B provided at least three disks are needed to cover B, as alluded to in the Introduction. Indeed, consider the Delaunay triangulation generated by the nodes in B^R. Because the centres of the Delaunay triangles are also covered, the edges of all Delaunay triangles are at most $2R$ units long, so they form part of the geometric graph we considered previously. So already the Delaunay triangulation, being a tessellation, tri-covers B. The converse is true only if trivial holes can be ignored. Formally, let $U = U(B)$ denote the event that a given convex set B is fully covered by disks, T be the event that B is fully tri-covered, and L and V – that there are points in B belonging to a large hole or a trivial hole, respectively. Then

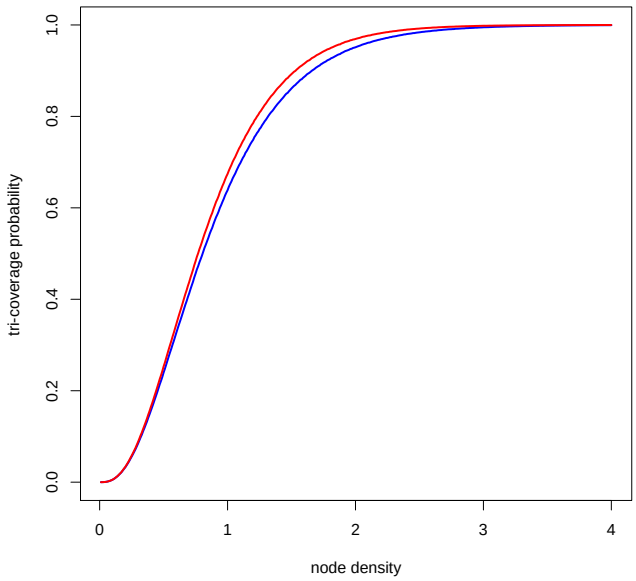

Fig. 7. Monte-Carlo estimated probability of tri-coverage (upper curve) and the lower bound given by (4) (lower curve).

$U(B^R) \subset U(B) \subset T(B)$ and $T \setminus U = V$. Therefore

$$\mathbf{P}(U(B^R)) \le \mathbf{P}(T) \le \mathbf{P}(U) + \mathbf{P}(V)\,. \tag{6}$$

Consider the case when B is a square of area b^2 and denote $a = \pi R^2$. As it follows by trivial scaling arguments from [9, Theorem 3.11], for any $\lambda > b^{-2}$ and all $0 < R < b/2$

$$0.05F(a,b,\lambda) < \mathbf{P}(U^{\mathbf{c}}) < 4F(a,b,\lambda)\,, \tag{7}$$

where[2]

$$F(a,b,\lambda) = \min\{1, (1 + ab^2\lambda^2)e^{-a\lambda}\}\,.$$

We are interested in the case where probability of full tri-coverage is close to 1, so it follows that the upper bound is of greatest importance for network design:

$$\mathbf{P}(T^{\mathbf{c}}) \le \mathbf{P}(U^{\mathbf{c}}(B^R)) \le 4F(a, b+R, \lambda)\,. \tag{8}$$

Thus if $\lambda = \lambda(B)$ is the density of nodes adjusted to B, then $b^2\lambda^2 e^{-a\lambda} \to 0$ with $\lambda \to \infty$ guarantees that the probability of finding a non-triangulated area in B also vanishes.

One can improve the bound (8) by noting that $T^{\mathbf{c}}$ means that there are points in B belonging to a large hole. Every such hole can be either formed by an isolated sensing area centred in B^R (i.e. not intersecting with any other such disks) or two intersecting disks isolated from the others, or it contains at least four exposed points (i.e. not covered by other disks) which lie at intersections between sensing disk boundaries (these are the corners of the white areas on Figure 1).

[2]There seems to be a small error in the original proof on p.181: the disks with centres less than 1 from the centre of $\mathcal{T}$ also contribute to variable M; this implies the constant 4 rather than 3 in the upper bound in (7).

TABLE I
ESTIMATED PROBABILITY OF TRI-COVERAGE $p(\lambda)$ FROM 10^6 MONTE-CARLO SIMULATIONS FOR DIFFERENT VALUES OF THE NODE DENSITY λ. THE ESTIMATED STANDARD ERROR IS 3.7×10^{-4}. ALSO ESTIMATED IS THE PROBABILITY THAT THERE IS TRI-COVERAGE INVOLVING THE CLOSEST NODE ξ_0 (`PROB.0`), AND THE PROBABILITY OF A TRIVIAL HOLE (`TRIV.HOLE`). THE ANALYTICAL BOUND (4) IS GIVEN IN THE COLUMN $p_0(\lambda)$.

λ	$p(\lambda)$	prob.0	triv.hole	$p_0(\lambda)$
0.1	0.005329	0.005327	0.000007	0.005735
0.2	0.033261	0.033203	0.000036	0.034677
0.3	0.087907	0.087678	0.000076	0.089330
0.4	0.164243	0.163722	0.000101	0.163168
0.5	0.253085	0.252174	0.000169	0.247864
0.6	0.346224	0.344848	0.000243	0.336143
0.7	0.437580	0.435858	0.000248	0.422615
0.8	0.525560	0.523393	0.000256	0.503749
0.9	0.605189	0.602860	0.000262	0.577533
1.0	0.674162	0.671494	0.000290	0.643079
1.1	0.734671	0.731986	0.000272	0.700268
1.2	0.785297	0.782631	0.000201	0.749469
1.3	0.828210	0.825595	0.000228	0.791327
1.4	0.863905	0.861508	0.000209	0.826625
1.5	0.892595	0.890303	0.000175	0.856179
1.6	0.915481	0.913352	0.000163	0.880786
1.7	0.934486	0.932563	0.000134	0.901181
1.8	0.948534	0.946837	0.000094	0.918028
1.9	0.960393	0.958836	0.000082	0.931907
2.0	0.969311	0.968036	0.000075	0.943322
2.1	0.976780	0.975663	0.000054	0.952699
2.2	0.982166	0.981225	0.000045	0.960399
2.3	0.986351	0.985527	0.000045	0.966721
2.4	0.989803	0.989114	0.000033	0.971915
2.5	0.992092	0.991509	0.000023	0.976188
2.6	0.994199	0.993721	0.000028	0.979709
2.7	0.995596	0.995185	0.000016	0.982616
2.8	0.996572	0.996244	0.000009	0.985023
2.9	0.997418	0.997151	0.000015	0.987021
3.0	0.998211	0.998014	0.000012	0.988686
3.1	0.998592	0.998426	0.000015	0.990079
3.2	0.998919	0.998792	0.000007	0.991248
3.3	0.999259	0.999154	0.000003	0.992235
3.4	0.999443	0.999355	0.000005	0.993072
3.5	0.999569	0.999504	0.000004	0.993785
3.6	0.999680	0.999625	0.000003	0.994396
3.7	0.999772	0.999728	0.000001	0.994921
3.8	0.999845	0.999812	0.000002	0.995377
3.9	0.999877	0.999845	0.000000	0.995773
4.0	0.999905	0.999888	0.000001	0.996120

The probability of existence of an isolated disk centred in B^R is at most the expected number of such disks. Therefore, by the Refined Campbell theorem,

$$\mathbf{E} \sum_{x\in\Pi\cap B^R} \mathbb{1}_{\Pi(b(x,2R))=1} = \lambda \int_{B^R} \mathbf{P}^x\{\Pi(b(x,2R))=1\}\,dx = \lambda(b+R)^2\, e^{-4\lambda a}\,,$$

where $\mathbf{P}^x$ is the local Palm distribution of Π, see, e. g., [16], (roughly speaking, the conditional distribution 'given there is a Π-point at x'). Similarly, for two isolated disks the bound is

$$\frac{1}{2}\,\mathbf{E} \sum_{x\in\Pi\cap B^R} \mathbb{1}_{\Pi(b(x,2R))=2} = 2\lambda^2 a(b+R)^2\, e^{-4\lambda a}\,.$$

Both bounds do not exceed $e^{-a\lambda}$ for sufficiently large λ.

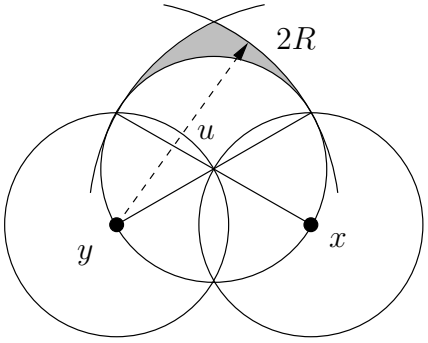

Fig. 8. Adding a ball with centre z inside the shaded zone would make a trivial hole, provided u is not covered by other balls not shown here.

In the third situation, the exposed intersection point $u = u(x,y)$ of two disks $b(x,R)$ and $b(y,R)$ has a zone $H(x,y,R) = b(x,2R)\cap b(y,2R)\setminus b(u,R)$ (shown shaded in Figure 8) which is free from nodes, otherwise such a node together with x and y would form a trivial hole rather than a large hole. Thus the existence of a large hole in the third situation implies that M, the number of exposed boundary intersection points with the above property, is at least 4, implying that

$$\mathbf{P}\{M\ge 4\} \le \frac{1}{4}\,\mathbf{E}\,M = \frac{1}{4}\lambda(b+R)^2 \times \int_{b(0,2R)} \mathbf{P}^0\{\Pi\big(b(u(0,y),R)\cup H(0,y,R)\big)=0\}\,\lambda dy$$

(When two disks intersect, they do so at two points, moreover each such point is counted twice when summation is carried out over all nodes). The area of $H(0,y,R)$ depends only on $r=\|y\|<2R$ and is equal to R^2 times

$$h(r) = \frac{r}{2}\Big[\sqrt{1-r^2/4}-\sqrt{4-r^2/4}\Big] + 3\arcsin(r/2) - 4\arcsin(r/4) \ge r^4/48\,.$$

Upon converting to polar coordinates, the integral above is smaller than

$$2a\sqrt{3\pi\lambda}\,\mathrm{erf}(\sqrt{\lambda/12})\,e^{-a\lambda}\,,$$

where $\mathrm{erf}(x) = \frac{2}{\sqrt{\pi}}\int_0^x e^{-t^2}dt < 1$. Combining everything, we see that for a fixed R and sufficiently large λ we have that

$$\mathbf{P}(T^{\mathbf{c}}) \le \Big[1+\frac{\sqrt{3\pi}}{2}\,a(b+R)^2\lambda^{3/2}\Big]\,e^{-a\lambda}\,. \qquad (9)$$

Comparing this with (8), even $b^2\lambda^{3/2}e^{-a\lambda}\to 0$ as above is sufficient to ensure that B has a high probability of being triangulated. The difference reflects the occurence of trivial holes which do not affect tri-coverage T, although they affect sensing coverage U.

V. Summary and Conclusions

In this paper, the concept of *tri-coverage* was used to approximate the proportion of sensing coverage in a wireless sensor network, assuming a two-dimensional Poisson process as a model of sensor node positioning. The principal analytical results require no assumptions to be made about the shape of the overall sensing area to be covered, and agree with the simulations very well, with a difference of just a few percent for all node densities. The bounds on the probabilities of both tri-coverage and also coverage of the whole target region are the key results of this paper because of their practical importance; in many deployment scenarios they will assist a network planner in estimating both the sensor node density which guarantees that at least a given proportion of the target sensing area is tri-covered, and also the order of sensor node density which ensures full sensing coverage. Furthermore, the concept of tri-coverage itself is directly relevant to the performance of a general class of distributed algorithms which run on the sensor nodes themselves, and which only require local connectivity information.

In order to provide full sensing coverage of a large area, the proportion of space which is tri-covered should be very close to 1, i.e. the sensor density λ should be large. Because of the computing time required, evaluating the sensing coverage for high λ through simulations becomes impractical. In contrast, our analytical bound presents no major technical difficulties and is very accurate.

To the best of the authors' knowledge, this is the first time that bounds on the probability of sensing coverage have been calculated analytically, without assumptions being made about the target area. These calculations suggest a fundamental framework for probabilistic coverage-based analysis using stochastic geometry, especially when seeking to evaluate the extent and quality of sensing coverage.

Finally, this paper also explored the relationship between tri-coverage and non-coverage, which is expressed by the probability of a trivial hole. Trivial holes account for only a tiny fraction of the total uncovered area, and hence may be ignored in practice when calculating coverage probabilities.

Acknowledgement

The authors are grateful to Claudia Redenbach for the short proof of tri-coverage implied by sensing coverage, which was presented at the beginning of Section IV. We also thank the anonymous reviewers for their thorough reading of draft versions of the paper, and for their detailed comments.

References

[1] B. N. Clark and C. J. Colbourn, "Unit disk graphs," *Discrete Mathematics*, vol. 86, no. 1-3, 1990.

[2] J. Dall and M. Christensen, "Random geometric graphs," *Physical Review E*, vol. 66, no. 1, 2002.

[3] M. Penrose, *Random Geometric Graphs*, ser. Oxford Studies in Probability. Oxford University Press, 2003.

[4] P. K. Biswas and S. Phoha, "Hybrid sensor network test bed for reinforced target tracking," in *Sensor Network Operations*, S. Phoha, T. LaPorta, and C. Griffin, Eds. Wiley, 2007, ch. 13, pp. 689–704.

[5] N. Ahmed, S. S. Kanhere, and S. Jha, "The holes problem in wireless sensor networks: a survey," *ACM SIGMOBILE Review*, vol. 9, no. 2, 2005.

[6] G. Kesidis, T. Konstantopoulos, and S. Phoha, "Surveillance coverage of sensor networks under a random mobility strategy," in *IEEE Sensors Conference*, Toronto, October 2003.

[7] S. Kumar, T. H. Lai, and J. Balogh, "On k-coverage in a mostly sleeping sensor network," *Tenth international Conference on Mobile Computing and Networking*, pp. 144–158, 2004.

[8] S. Janson, "Random coverings in several dimensions," *Acta Math.*, vol. 156, pp. 83–118, 1986.

[9] P. Hall, *Introduction to the Theory of Coverage Processes*. Wiley, 1988.

[10] H. Zhang and J. Hou, "On deriving the upper bound of α-lifetime for large sensor networks," *Fifth ACM International Symposium on Mobile Ad-hoc Networking and Computing*, 2004.

[11] X. Li and D. K. Hunter, "Distributed coordinate-free algorithm for full sensing coverage," *International Journal of Sensor Networks*, 2009.

[12] Y. Bejerano, "Efficient k-coverage verification without location information," *IEEE INFOCOM*, 2008.

[13] S. Zuyev, "Stopping sets: Gamma-type results and hitting properties," *Adv. in Applied Probab.*, vol. 31, no. 2, pp. 355–366, 1999.

[14] R. Cowan, M. Quine, and S. Zuyev, "Decomposition of Gamma-distributed domains constructed from Poisson point processes." *Adv. in Applied Probab.*, vol. 35, no. 1, pp. 56–69, 2003.

[15] R Development Core Team, *R: A Language and Environment for Statistical Computing*, R Foundation for Statistical Computing, Vienna, Austria, 2008, ISBN 3-900051-07-0. [Online]. Available: http://www.R-project.org

[16] D. J. Daley and D. Vere-Jones, *An Introduction to the Theory of Point Processes. Volume I: Elementary Theory and Methods*, 2nd ed. New York: Springer, 2003.

Xiaoyun Li is an Associate Professor with Center for Intelligent and Biomimetric Systems, Center for Intelligent Sensors at Shenzhen Institute of Advanced Technology (SIAT) in the Chinese Academy of Science. He was awarded an M.Sc. degree in Computer and Information Networks from the Department of Computing and Electronic Systems at the University of Essex, UK in 2004, and graduated with a Ph.D. from the same department in 2008 for research on wireless sensor networks. He worked as a postdoctoral research fellow at both University College Dublin and the University of Essex from 2008 until 2011. His research interests include MAC protocols such as IEEE 802.15.4 and positioning algorithms.

David K. Hunter is a Reader in the Department of Computing and Electronic Systems in the University of Essex. In 1987, he obtained a first class honours B.Eng. in Electronics and Microprocessor Engineering from the University of Strathclyde, and a Ph.D. from the same university in 1991 for research on optical TDM switch architectures. After that, he researched optical networking and optical packet switching at Strathclyde. He moved to the University of Essex in August 2002, where his teaching concentrates on TCP/IP, network performance modelling and computer networks. He has authored or co-authored over 130 publications. From 1999 until 2003 he was an Associate Editor for the IEEE Transactions on Communications, and he was an Associate Editor for the IEEE/OSA Journal of Lightwave Technology from 2001 until 2006. He is a Chartered Engineer, a Member of the IET, a Senior Member of the IEEE and a Professional Member of the ACM.

Sergei Zuyev graduated in 1984, and received his PhD in Mathematical and Physical Sciences from the Mechanics and Mathematics faculty of Moscow State University in 1988. In 1992–1998 he worked in INRIA, France, in the framework of Convention with France Telecom on Modelling of Complex Telecommunication Systems. From 1998 until 2009, he was a Reader at the University of Strathclyde. He was the Principal Investigator in a major UK Research Council Grant on Modelling and Analysis of Future Broadband Communications Networks and has co-authored numerous research papers on probability, statistics and telecommunications. Since 2009, he has held a Chair in Mathematical Statistics at Chalmers University of Technology, Sweden.